Structure of 1-Naphthol/Alcohol Clusters Studied by IR Dip Spectroscopy and ab Initio Molecular Orbital Calculations

Morihisa Saeki, Shun-ichi Ishiuchi, Makoto Sakai, and Masaaki Fujii*

Institute for Molecular Science/Graduate School for Advanced Study, Myodaiji, Okazaki 444, Japan

Received: April 3, 2001; In Final Form: July 19, 2001

The structures of 1-naphthol/alcohol clusters, 1-NpOH(ROH)$_n$ ($n = 1-3$; ROH = MeOH, EtOH, and *t*-BuOH), have been investigated by resonant two-photon ionization (R2PI) spectroscopy and ion-detected IR dip spectroscopy. On the basis of the calculated spectra obtained by ab initio MO calculations, the spectra of 1-NpOH(MeOH)$_n$ was analyzed. The analysis elucidated that 1-NpOH(MeOH)$_{2,3}$ was a ring structure. From a similarity of the spectral pattern, the structures of 1-NpOH(EtOH)$_n$ and 1-NpOH(*t*-BuOH)$_n$ were also determined to be a ring conformation. From a frequency shift of the hydrogen-bonded OH stretching vibration, the hydrogen bonding is weakened by a steric hindrance due to an alkyl group of ROH. The difference in the solvation mechanism between 1-NpOH(MeOH)$_n$ and 1-NpOH(H$_2$O)$_n$ is discussed.

I. Introduction

It is known that photoexcited phenol and naphthols become highly acidic and donate their proton to a solvent.[1−10] This phenomenon, which is called excited-state proton transfer (ESPT), has been widely investigated and reviewed in a condensed phase.[11,12] Especially, 1-naphthol (1-NpOH) shows a large change in acidity in the excited state. A weak base in its electronic ground state, S_0 ($pK_a = 9.4$), becomes a strong acid in its S_1 excited state ($pK_a = 0.5 \pm 0.2$).[6,7] The ESPT of 1-NpOH in aqueous solutions was first investigated by Förster[8] and later by Weller.[9,10] The primary diagnostic criterion of the ESPT is emission. In solution, the undissociated 1-NpOH* emits weak fluorescence in the wavelength rage of 320−380 nm, while the naphtholate anion (1-NpO$^-$*) is characterized by a red-shifted (≈7000 cm^{-1}) broad emission band in the range of 400−500 nm. Thus, the appearance of the red-shifted broad emission band indicates the occurrence of ESPT. In a bulk water solution at room temperature, the emission of 1-NpO$^-$* is predominant,[6−10] while only molecular 1-NpOH* emission is observed in methanol.[13] These results showed that the dynamics in the excited state is different between the water and methanol solution. Similarly, the ESPT of 1-NpOH was also observed in a glass-forming solvent.[14]

The ESPT in a microsolvent cluster was first observed by Cheshovsky and Leutwyler.[15] They observed the fluorescence emission spectra of 1-NpOH solvated by ammonia, 1-NpOH-(NH$_3$)$_n$, and found the appearance of red-shifted broad emission centered at 24400 cm^{-1}. Following the first observation of ESPT in the cluster, the structures and reactions of 1-NpOH solvated by various polar molecules, such as 1-NpOH(H$_2$O)$_n$, 1-NpOH-(MeOH)$_n$, 1-NpOH(NH$_3$)$_n$, and 1-NpOH(piperidine)$_n$, have been studied by dispersed fluorescence,[16−19] resonant enhanced multiphoton ionization,[20−27] IR dip spectroscopy,[28] rotational coherence spectroscopy,[29] and ultrafast measurement.[30−37] The study in these clusters showed that ESPT occurs in 1-NpOH-(piperidine)$_2$,[16] 1-NpOH(NH$_3$)$_4$,[15,16,20,24−27] and 1-NpOH(H$_2$O)$_n$ ($n \geq \sim 30$),[21] although it has not been observed in 1-NpOH-(MeOH)$_n$ ($n \geq 8$).[16] The nonobservation of the ESPT in a 1-NpOH(MeOH)$_n$ cluster is consistent with the experimental result in the condensed phase.

To understand the mechanism of ESPT, the proton affinity (PA) has been employed as a scale of reactivity.[16,21] From this point, the absence of ESPT in a 1-NpOH(MeOH)$_n$ cluster is exceptional because PA of MeOH is between H$_2$O and NH$_3$, and it is larger than the proposed reaction threshold (PA = 243 kcal/mol). It suggests that the 1-NpOH(MeOH)$_n$ cluster contains new information on the mechanism of ESPT.

In this work, to elucidate the different solvation mechanisms of alcohols including MeOH and other polar solvents, we studied the structures of 1-NpOH/alcohol clusters, 1-NpOH(ROH)$_n$ (ROH = MeOH, EtOH, and *t*-BuOH). The gas-phase PA increases in the sequence H$_2$O < MeOH < EtOH < *t*-BuOH < NH$_3$ < piperidine.[38] A study about a series of alcohol solvents enabled us to systematically discuss a change in the solvation mechanism in connection with the PA. We have investigated the geometric structures using an ion-detected IR dip spectroscopy, which is widely used to measure the IR spectra of the clusters.[39−41] First, we measured the resonant two-photon ionization (R2PI) spectra of 1-NpOH(ROH)$_n$ to learn about the electronic origin band in $S_1 \leftarrow S_0$ excitation. We then showed the IR dip spectra of 1-NpOH(ROH)$_n$ by using the electronic origin bands. To analyze the IR spectra of 1-NpOH(ROH)$_n$, optimized geometries and theoretical IR spectra were obtained for 1-NpOH(MeOH)$_n$ by ab initio MO calculations. From a comparison of the observed and calculated IR spectra, the structures of the 1-NpOH(MeOH)$_n$ were determined. On the basis of the obtained structures in 1-NpOH(MeOH)$_n$, the IR spectra of 1-NpOH(EtOH)$_n$ and 1-NpOH(*t*-BuOH)$_n$ were analyzed. Finally, on the basis of the structure in 1-NpOH/alcohol clusters, the difference in the solvation mechanism of 1-NpOH-(MeOH)$_n$ and 1-NpOH(H$_2$O)$_n$ is discussed.

II. Methods

A. Experimental Method. A detailed description of the experimental setup for R2PI and ion-detected IR dip spectroscopy is presented elsewhere.[28,42] The 1-NpOH(ROH)$_n$ were generated by a supersonic expansion of 1-NpOH (Tokyo Kasei)

* Author to whom correspondence should be addressed.

10.1021/jp0112469 CCC: $20.00
Published on Web 10/13/2001

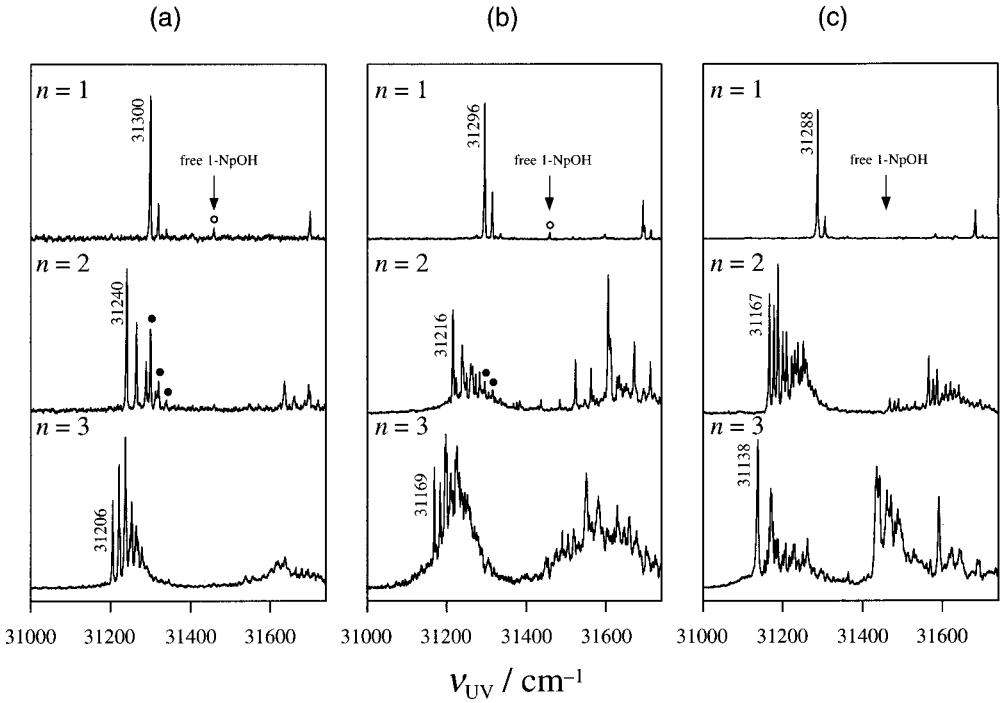

Figure 1. Resonant two-photon ionization spectra of 1-NpOH(ROH)$_n$ (n = 1−3; R = Me, Et and *t*-Bu). An arrow indicates the position of the electronic origin of monomer. The peaks marked by an open circle, ○, are assigned the bands of 1-NpOH, which appear because an ionized 1-NpOH cluster accompanies a ROH molecule floating in free-jet condition. The peaks marked by a solid circle, ●, are assigned the bands of 1-NpOH(ROH), which is produced by the same phenomenon. The appearance of those peaks depends on the experimental condition.

vapor at 360 K seeded in He gas at 2−2.5 atm, which contained alcohol vapor at 243−258 K. The pulsed nozzle was operated at 20 Hz. The R2PI measurements were carried out using the frequency-doubled output of a dye laser (Lumonics HD-500 with DCM dye) pumped by the third harmonics of a Nd^{3+}:YAG laser (Spectra Physics GCR 170). The molecules or clusters ionized by the UV laser were detected by a channel multiplier (Murata Ceratron) through a quadrupole mass filter (Extrel). The signal was amplified by a preamplifier (PAR113) and then integrated by a digital boxcar system (EG&G PARC model 4420/4422). The integrated signal was recorded by a personal computer (NEC PC 9801) as a function of the UV laser frequency.

When the IR spectra of the solvated clusters were measured, the frequency of the UV laser was fixed to the S_1 origin of a specific cluster. The intensity of the R2PI signal generated by the UV laser is in proportion to the population of the cluster. The IR laser irradiates the cluster prior to irradiation of the UV laser and scans in the energy region from 2950 to 3750 cm^{-1}. When the frequency of the IR laser matches the transition to a certain vibrational level, the ion current decreases because of a loss of population from the ground vibrational state. As a result, the vibrational transition is detected as a depletion of the ion current. A tunable pulsed IR laser was generated by a difference-frequency mixing between a second harmonic of an injection-seeded Nd^{3+}:YAG laser (HOYA Continuum Powerlite 8010) and a YAG pumped dye laser (Lumonics HD-500) with a $LiNbO_3$ crystal. Both the IR laser and the UV laser were focused by lenses (f = 250 mm) and were coaxially introduced into a vacuum chamber and crossed a supersonic jet. The time delay between the IR laser and the UV laser was 50 ns. The timing between the two lasers was adjusted by a digital delay generator (Stanford Research DG-535). We employed alternative data acquisition to improve signal-to-noise ratio. The UV laser was operated at 20 Hz, while the IR laser was operated at 10 Hz. The signal due to IR + UV and that due to UV only appeared alternatively. Each signal was integrated separately by a digital boxcar. As a result, we could monitor the ion current without the IR laser (background). We obtained normalized spectra by dividing the background into the dip spectra.

B. Calculation. The molecular structures of 1-NpOH-(MeOH)$_n$ (n = 1−3) were optimized using an energy-gradient technique for the second-order many-body perturbation method (MP2) with the usual frozen-core approximation. The basis set used was the standard 6-31G basis set. A vibrational analysis using an analytical second-derivative matrix was carried out to characterize the nature of the stationary points. If the optimized structure had one or more imaginary frequencies, we further optimized the structure until the true local minimum structure was obtained, where all of the vibrational frequencies are real. The IR intensities for the vibrations were evaluated for all minimum energy structures. The total hydration enthalpies at 0 K were computed with the calculated harmonic frequencies without scaling. All of the computations were carried out on an NEC SX-5 computer at the Computer Center of the Institute for Molecular Science (IMS). The program used was GAUSSIAN 98.[43]

III. Results and Discussion

A. R2PI Spectra of 1-NpOH(ROH)$_n$. Figure 1a−c shows the $S_1 \leftarrow S_0$ mass-selected R2PI spectra of 1-NpOH(MeOH)$_n$, 1-NpOH(EtOH)$_n$, and 1-NpOH(*t*-BuOH)$_n$ (n = 1−3) within the region of 31000−31750 cm^{-1}, respectively. The size-selected electronic spectra of these solvated clusters were measured in a supersonic jet for the first time, except for 1-NpOH(MeOH)$_1$.[23] The wavenumber of the electronic origins of respective clusters are indicated by the numeric label in the figure. The position of the electronic origin of free *trans*-1-NpOH at ν = 31458 cm^{-1} is also indicated by an arrow. Although there are two rotational isomers in the 1-NpOH monomer, namely *trans*- and *cis*-1-NpOH, we mention only *trans*-1-NpOH, because the population of *cis*-1-NpOH is negligible.[22,44] In every spectrum

TABLE 1: Values of the Red-Shift of the Origin Band of 1-NpOH(ROH)$_n$ from That of 1-NpOH Monomer, Together with the Gas-Phase PA of ROH Monomer

	$\Delta\nu$ (cm^{-1})			
solvent	$n = 1$	$n = 2$	$n = 3$	PA (kcal/mol)
MeOH	158	218	252	184.9[a]
EtOH	162	242	289	190.3[a]
t-BuOH	170	291	320	195[a]

[a] Ref 38.

shown in Figure 1a−c, sharp absorption bands were observed, consisting of a strong electronic origin and associated excited-state vibronic bands. As the clusters increase in size, the electronic origins shift monotonically to the red. The spectral shifts of the electronic origins relative to the free 1-NpOH origin, $\Delta\nu$, are listed in Table 1, along with their PA of the monomer. The shift $\Delta\nu$ of the $n = 1$ cluster increases with increasing PA. This tendency is also true for clusters with $n = 2$ and 3.

In clusters with $n = 1$, all R2PI spectra show low-frequency vibrational bands. The spacings between the vibrational bands are 20 cm^{-1}, 19 cm^{-1}, and 18 cm^{-1} in MeOH, EtOH, and *t*-BuOH, respectively. Because these bands have not been observed in the $S_1 \leftarrow S_0$ transition of bare 1-NpOH, the vibrational mode is attributed to a low-frequency intermolecular mode. We tentatively assigned it as out-of-plane bending vibration of the solvent based on the analogy of PhOH(H$_2$O)$_1$.[45] The spectra of the clusters with $n \geq 2$ showed many vibrational features with strong intensities, which is in contrast with the spectra in $n = 1$, where the electronic origin band is dominant. Especially, 1-NpOH(MeOH)$_3$, 1-NpOH(EtOH)$_3$, and 1-NpOH-(*t*-BuOH)$_2$, clearly show stronger intermolecular bands than the origin. This suggests a significant change in the geometries by $S_1 \leftarrow S_0$ electronic excitation for these clusters.

B. IR Dip Spectra of 1-NpOH(MeOH)$_n$. The IR dip spectra of 1-NpOH(MeOH)$_n$ ($n = 1-3$) are shown in Figure 2. The IR dip spectra of the monomer are also shown in the figure for comparison. The observed frequencies of the vibrational bands are listed in Table 2. All spectra were obtained by fixing the UV laser to the S_1 origin of each species. The IR dip spectrum of 1-NpOH(MeOH)$_1$ showed two dips at 3437 and 3680 cm^{-1}. Because the frequencies are obviously higher than that of CH stretching vibration (∼3000 cm^{-1}), the bands at 3437 and 3680 cm^{-1} are assignable to the OH stretching vibration of the cluster. Because the observed frequency of 3680 cm^{-1} is close to the OH stretching vibrations in MeOH (3682 cm^{-1}),[46] the latter is assigned to the OH stretching vibrations of the MeOH moiety. As a result, the band at 3437 cm^{-1} can be assigned to OH stretching in 1-NpOH. This assignment is consistent with the fact that the frequency of the OH stretching vibration of the proton donor is known to decrease in hydrogen-bonded clusters.[39,41,47−60] We concluded that 1-NpOH is a proton donor and that MeOH is a proton acceptor in 1-NpOH(MeOH)$_1$.

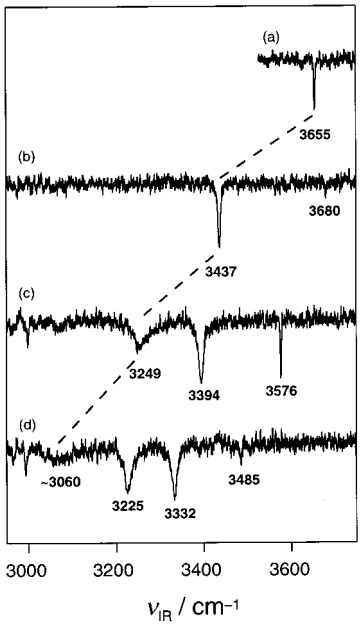

Figure 2. IR dip spectra of (a) 1-NpOH, (b) 1-NpOH(MeOH), (c) 1-NpOH(MeOH)$_2$, and (d) 1-NpOH(MeOH)$_3$.

The 1-NpOH(MeOH)$_2$ shows three bands, while 1-NpOH-(MeOH)$_3$ shows four bands: three strong bands in the region from 3200 to 3700 cm^{-1} and one broad band at ∼3060 cm^{-1}. Because of their frequencies, the bands should also be assigned to OH stretching vibrations. The band at the lowest frequency (3249 and ∼3060 cm^{-1} for $n = 2$ and 3, respectively) is tentatively assigned to νOH of 1-NpOH in each cluster. Other bands (at 3394 and 3576 cm^{-1} for $n = 2$; at 3225, 3332, and 3485 cm^{-1} for $n = 3$) are assigned to an OH stretching vibration of the hydrogen-bonded OH group of the MeOH moieties in the clusters (H-bonded OH stretch). Detailed assignments are discussed in Section III.D., on the basis of a comparison with the theoretically calculated system.

C. Optimized Structures of 1-NpOH(MeOH)$_n$ ($n = 1-3$). The optimized structures of 1-NpOH(MeOH)$_n$ ($n = 1-3$) are shown in Figure 3, together with the structure of 1-NpOH monomer. Yoshino et al. compared the calculated vibrational frequencies of 1-NpOH(H$_2$O)$_n$ at the MP2/6-31G level with the experimental one, and found a good agreement between them.[28] Because a structural comparison of 1-NpOH(H$_2$O)$_n$ and 1-NpOH-(MeOH)$_n$ is needed, we also performed a calculation at the MP2/6-31G level. For the size with $n = 1$, we have found two isomers: **1a** and **1b**. In structure **1a**, the O−H bond length in the 1-NpOH is elongated by ∼0.01 Å. On the other hand, the

TABLE 2: Observed and Calculated OH Stretching Frequencies (cm^{-1}) of 1-NpOH Monomer, 1-NpOH(MeOH)$_n$ ($n = 1-3$) Clusters, and MeOH Monomer

	observed frequencies		calculated frequencies	
	1-NpOH moiety νOH(1-NpOH)	MeOH moiety νOH(MeOH)	1-NpOH moiety νOH(1-NpOH)	MeOH moiety νOH(MeOH)
trans-1-NpOH	3655		3640	
1-NpOH(MeOH)	3437	3680	3396	3697
1-NpOH(MeOH)$_2$	3249	3394	3210	3386
		3576		3525
1-NpOH(MeOH)$_3$	∼3060	3225	2939	3152
		3332		3272
		3485		3388
MeOH		3682[a]		3659

[a] Ref 46.

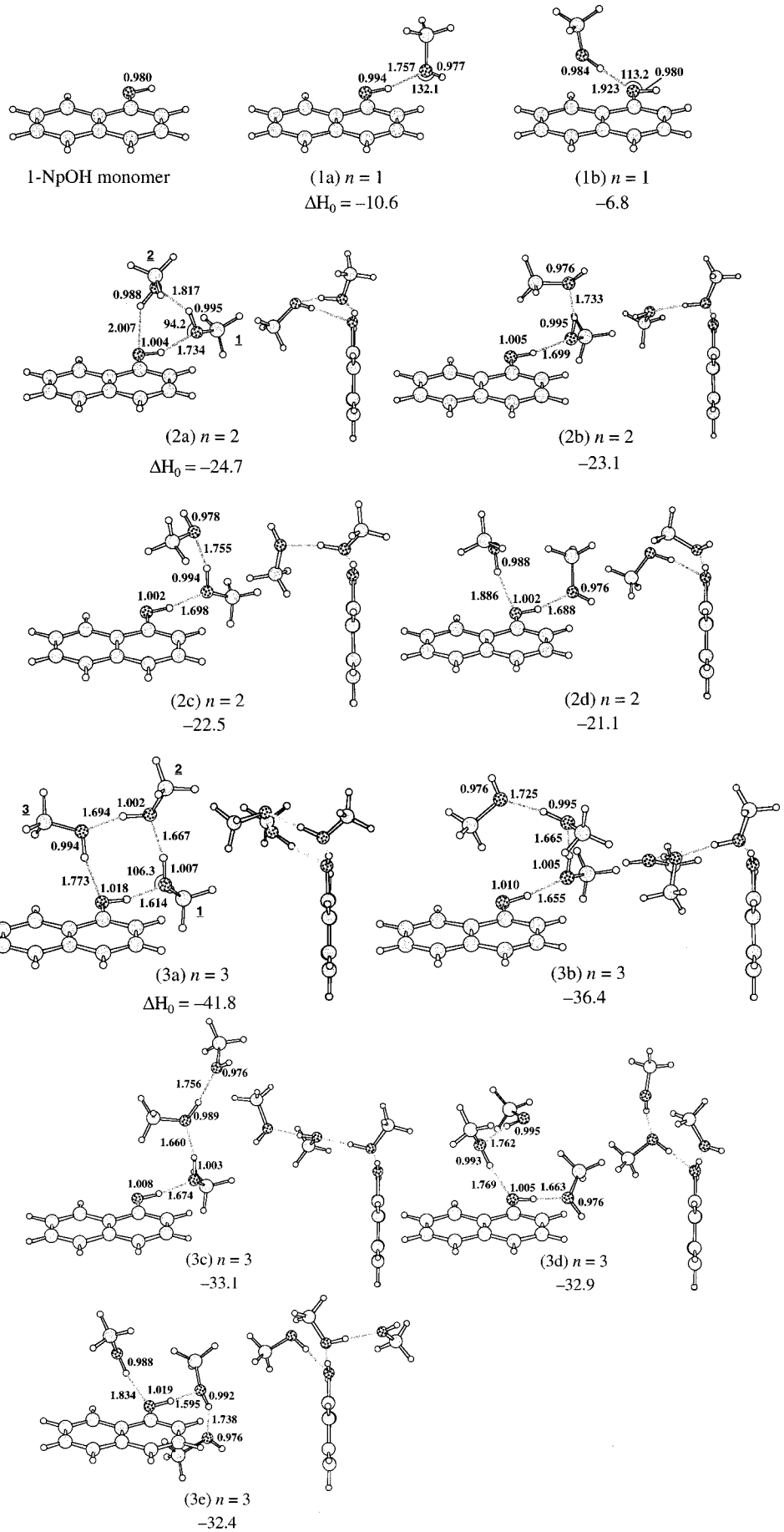

Figure 3. Optimized structures of 1-NpOH(MeOH)$_n$ (n = 1−3) at MP2/6-31G level, together with the structure of 1-NpOH monomer. Bond lengths are given in angstrom. Calculated total hydration enthalpies at 0 K (ΔH_0) are also presented in kcal/mol.

O−H bond length in MeOH does not change much by forming the cluster (0.979 Å at MP2/6-31G level) for free MeOH. This indicates that the 1-NpOH is a proton donor and that MeOH is a proton acceptor. The hydrogen bond is formed by an interaction of the lone electron pair on the O atom of the MeOH and the H atom of the OH moiety of 1-NpOH. Structure **1a** shows that an adequate H−O−H angle for the formation of a hydrogen bond between 1-NpOH and free MeOH is 132.1°, which is regarded as the direction of the lobe of the lone electron-pair on the O atom. The methyl group of MeOH is attracted by aromatic ring of 1-NpOH, which is the case with phenol/methanol complex.[61,62] A strong interaction between MeOH and the aromatic ring is suggested in 1-NpOH(MeOH) as well as phenol/methanol complex. The optimized geometry in structure **1b** showed that the MeOH is a proton donor, while the 1-NpOH is a proton acceptor. Here, the O−H bond length in the MeOH is elongated by 0.005 Å, while that in the 1-NpOH is the same with an isolated 1-NpOH monomer. The intermolecular distance in structure **1b** is longer than that in structure **1a** by ∼0.17 Å. This indicates that the intermolecular interaction between 1-NpOH and MeOH in structure **1a** is stronger than that in structure **1b**. Structure **1a** is calculated to be more stable than structure **1b** by 3.8 kcal/mol. The tendency in relative stability between isomers is similar with the case of 1-NpOH-$(H_2O)_1$.[28]

For the size with $n = 2$, four isomers have been found. The most stable isomer, structure **2a**, has a ring structure formed by two MeOH and the OH of 1-NpOH, the latter being both a proton acceptor and a donor. The intermolecular distance between the 1-NpOH and the MeOH accepting the proton of the 1-NpOH is shorter than that in structure **1a** by 0.023 Å. The H−O−H angle in the 1-NpOH and the MeOH accepting the proton is 94.2°, which is much less than the adequate angle, 132.1°. Thus, the O−H···O hydrogen bond is bent in the 1-NpOH$(MeOH)_2$. This indicates that the hydrogen-bonded network is deformed for forming the ring structure. In structures **2b** and **2c**, which are less stable than structure **2a**, a hydrogen-bonded chain of MeOH is formed. The methyl group of the terminal MeOH is located on the O atom of 1-NpOH in structure **2b**, while that of structure **2c** heads for the π-system of 1-NpOH. In structure **2d**, the OH of 1-NpOH acts both as a proton donor and a proton acceptor, where a hydrogen bond is not formed between the MeOH acting as a proton acceptor and a proton donor. The calculated results showed that the structures of 1-NpOH$(MeOH)_2$ can be classified into three types; (i) a ring structure, (ii) a chain structure, and (iii) a structure with no interaction between two MeOH solvents. In the case of the 1-NpOH$(MeOH)_2$ cluster, the ring structure is most stable.

For the size with $n = 3$, five isomers have been found. The most stable isomer of the 1-NpOH$(MeOH)_3$ cluster is **3a**, having a ring structure. Comparing structures **3a** with **2a**, the intermolecular distance is shortened, while the bond length of every OH is elongated. The H−O−H angle in the 1-NpOH and the MeOH accepting the proton is 106.3°, which approach an adequate angle. The bending of the O−H···O hydrogen bond in 1-NpOH$(MeOH)_3$ is smaller than that in 1-NpOH$(MeOH)_2$. This is attributed to the formation of a larger hydrogen-bonded ring in 1-NpOH$(MeOH)_3$, which reduces the deformation of the hydrogen-bonded network. Structures **3b** and **3c** have a chain structure. Structure **3b** is formed by attaching one MeOH to structure **2c**, while structure **3c** comes from structure **2b**. In structure **3b**, the methyl group of the terminal MeOH heads for the π-system of the 1-NpOH. In structures **3d** and **3e**, the OH of 1-NpOH acts both as a proton donor and a proton acceptor,

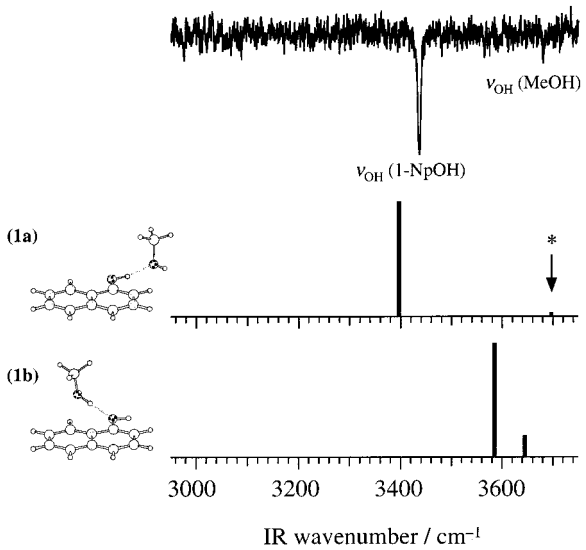

Figure 4. Calculated IR spectra of 1-NpOH(MeOH) for the optimized structures **1a**−**1b**. The structures are illustrated beside the calculated spectra. The observed IR dip spectrum is also shown on top.

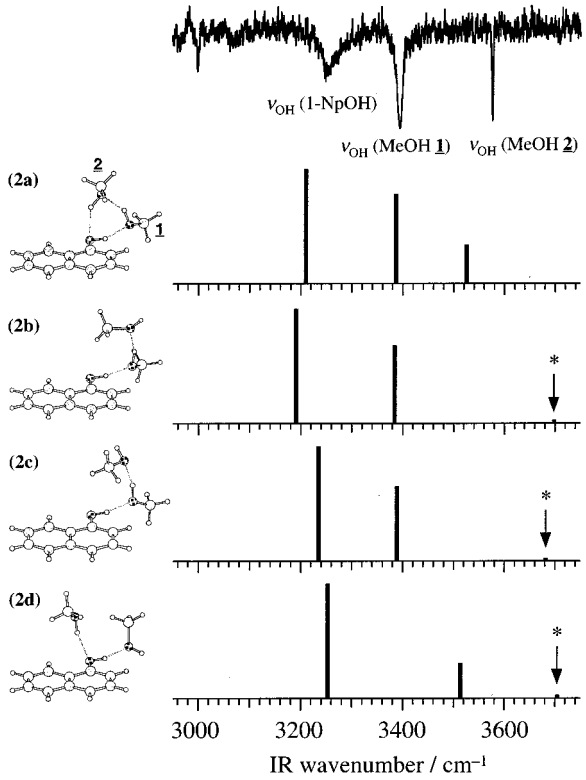

Figure 5. Calculated IR spectra of 1-NpOH$(MeOH)_2$ for the optimized structures **2a**−**2d**. The structures are illustrated beside the calculated spectra. The observed IR dip spectrum is also shown on top.

where a hydrogen bond is not formed between the MeOH acting as a proton acceptor and a proton donor. Structure **3d** is constructed by attaching one MeOH to another MeOH acting as a proton acceptor, while structure **3e** is constructed by attaching to the MeOH acting as a proton donor. As is the case with $n = 2$, the ring structure is most stable.

D. Assignment of the Bands of 1-NpOH$(MeOH)_n$ (n = 1−3). In this section, we examine the assignment of the bands in the IR dip spectra and determine the structures of 1-NpOH-$(MeOH)_n$. The calculated IR spectra are shown in Figures 4−6, together with the observed spectrum. Only the frequencies being attributed to the OH vibration are displayed, because the

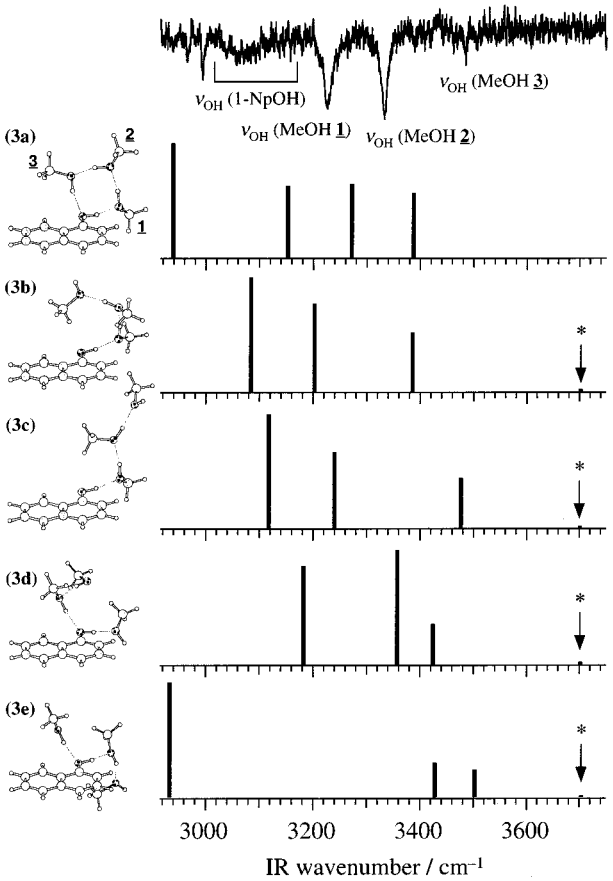

Figure 6. Calculated IR spectra of 1-NpOH(MeOH)$_3$ for the optimized structures **3a**−**3e**. The structures are illustrated beside the calculated spectra. The observed IR dip spectrum is also shown on top.

frequencies of the other modes (CH stretching of 1-NpOH and MeOH) are not sensitive to a structural change of the cluster. At the MP2/6-31G level, the harmonic frequencies of the OH stretching vibrations of the 1-NpOH and MeOH monomer were computed to be 3640 and 3659 cm^{-1}, respectively. In the spectrum for structure **1a** (Figure 4), there is one strong band and one weak band at 3396 and 3697 cm^{-1}. Their relative IR intensities are 1.00 and 0.03, respectively. The calculated normal mode corresponding to the band at 3396 cm^{-1} is the OH stretching of 1-NpOH, and the band at 3697 cm^{-1} is attributed to the stretching vibration of the OH bond in MeOH. Hereafter, the vibrational bands of 1-NpOH and MeOH are denoted as νOH(1-NpOH) and νOH(MeOH), respectively. In spectrum **1b**, we can also see two bands whose relative intensities are 1.00 and 0.19, respectively. Their normal modes are the vibrations of the hydrogen-bonded MeOH (3585 cm^{-1}) and 1-NpOH (3645 cm^{-1}). The νOH(1-NpOH) remained almost unchanged from that of the free 1-NpOH, since the OH bond is free from the hydrogen bond in **1b**. It is interesting to note that the MeOH band was calculated to be more intense than the νOH(1-NpOH) band. By comparing the two calculated spectra with the experimental one, we can easily note that the observed spectrum is better reproduced by **1a** than by **1b**. Therefore, we have concluded that the observed spectrum can be attributed to a structure in which 1-NpOH is a proton donor, and have confirmed a tentative assignment of the observed bands in Section III.B. In the spectrum of 1-NpOH(MeOH), the νOH-(1-NpOH) band is red-shifted due to proton donation of the OH group in the hydrogen bond. On the other hand, the frequencies of νOH(MeOH) remained almost unchanged from that of the free MeOH. These facts indicate that the vibrational nature of MeOH is not very much affected by complex formation. In addition, the MeOH band is much weaker than the νOH(1-NpOH) band. The calculated frequency of νOH(1-NpOH) underestimates the experiment only by 1.2% and that of νOH-(MeOH) overshoots by 0.4%. The theoretical IR spectra of structures **2a**−**2d** are shown in Figure 5, together with the observed IR dip spectrum for 1-NpOH(MeOH)$_2$. We note that the calculated spectrum for **2a** agrees with the experimental results much better than others. The spectrum of structure **2a** shows three strong bands, while there are two strong bands and one weak band in structures **2b**−**2d**. The calculated normal mode corresponding to the weak band (about 3700 cm^{-1}, indicated by an asterisk) in structures **2b**−**2d** is the free OH stretching of MeOH, which is absent in the observed spectrum. Thus, we should rule out structures **2b**−**2d** and conclude that the structure of 1-NpOH(MeOH)$_2$ is **2a**. The computational results showed that the motion of each OH vibrational mode in **2a** is mainly localized in a single OH bond. The OH stretching motion of 1-NpOH is almost the dominant contributor to the lowest vibrational band. We can thus call the band at 3249 cm^{-1} νOH(1-NpOH). Similarly, the second lowest (at 3394 cm^{-1}) and the highest OH bands (at 3576 cm^{-1}) can be described by the localized motion in the first and second MeOH molecules νOH(MeOH ***1***) and νOH(MeOH ***2***). Quantitatively speaking, the calculation underestimates the frequencies of νOH(1-NpOH) and the H-bonded OH stretch by at most 0.2−2.2%. The νOH-(1-NpOH) band is further shifted to the red from $n = 1$ by ∼188 cm^{-1}. To sum up we have concluded that the 1-NpOH(MeOH)$_2$ cluster has the ring structure, and have confirmed tentative assignments of the observed bands given in the previous section.The calculated IR spectra for the four structures of 1-NpOH(MeOH)$_3$ are shown in Figure 6. This figure clearly indicates that structure **3a** is the best candidate among the isomers examined for the observed IR dip spectrum for $n = 3$. Only **3a** shows the four strong bands near the observed dips. In addition, the absence of the bands of free MeOH is also well reproduced only by this cluster. The four bands correspond to the vibrations of the H-bonded OH groups in the ring. As is the case with 1-NpOH(MeOH)$_2$, the calculated frequencies are mainly attributed to a local mode. The lowest band (∼3060 cm^{-1}) can be regarded as the OH vibration of the 1-NpOH modified by hydration, and the three middle bands are the vibrations of the H-bonded OH groups of the MeOH forming the ring structure. Therefore, we can assign the observed strong band at 3205 cm^{-1} to νOH(1-NpOH), and the next three bands to the H-bonded OH stretch. The bands at 3248, 3316, and 3548 cm^{-1} are assigned to νOH(MeOH ***1***), νOH(MeOH ***2***), and νOH-(MeOH ***3***), respectively. The calculated frequencies of νOH-(1-NpOH) are lower than the observed values by ∼4%, while the other theoretical OH frequencies differ from the experimental value by 1.8−2.8%. We note that the difference between the observed and calculated frequencies of νOH(1-NpOH) in 1-NpOH(MeOH)$_n$ increases as n grows, which is similar to those in 1-NpOH(H$_2$O)$_n$. From the energy relationship among isomers and their vibrational spectral features, we have concluded that 1-NpOH(MeOH)$_3$ has a ring structure (**3a**) with an eight-membered ring. All of the observed and calculated frequencies of the OH vibrations and their assignments are summarized in Table 2.

E. IR Dip Spectra of 1-NpOH(EtOH)$_n$ and 1-NpOH(*t*-BuOH)$_n$. The IR dip spectra of 1-NpOH(ROH)$_n$ ($n = 1-3$; R = Et, *t*-Bu) are shown in Figure 7, together with the spectrum of 1-NpOH(MeOH)$_n$. The observed frequencies are listed in Table 3. All of the IR dip spectra with $n = 1$ show one strong

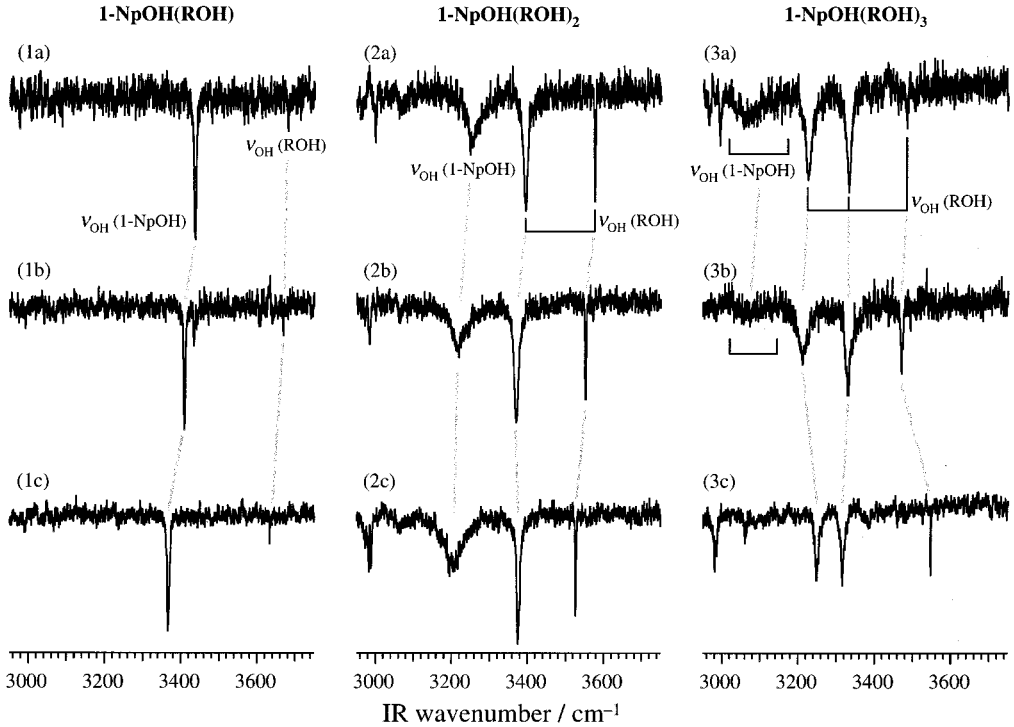

Figure 7. IR dip spectra of (1a−c) 1-NpOH(ROH) (R = Me, Et, and *t*-Bu), (2a−c) 1-NpOH(ROH)$_2$ (R = Me, Et, and *t*-Bu), (3a−c) 1-NpOH(ROH)$_3$ (R = Me, Et, and *t*-Bu).

TABLE 3: Observed OH Stretching Frequencies (cm^{-1}) of 1-NpOH(EtOH)$_n$ and 1-NpOH(*t*-BuOH)$_n$ (n = 1−3)

	R = Et		R = *t*-Bu	
	1-NpOH moiety νOH(1-NpOH)	alcohol moiety νOH(ROH)	1-NpOH moiety νOH(1-NpOH)	alcohol moiety νOH(ROH)
1-NpOH(ROH)	3409	3668	3366	3633
1-NpOH(ROH)$_2$	3215	3369	3199	3375
		3552		3526
1-NpOH(ROH)$_3$	∼3060	3221		3248
		3330		3316
		3471		3548

band in the region 3350−3450 cm^{-1}, and one weak band in 3670−3700 cm^{-1}. Assuming that the 1-NpOH is a proton donor and that the solvent is a proton acceptor, which is the case for 1-NpOH(MeOH)$_1$, both the strong band and the weak one can be assigned to H-bonded νOH of the 1-NpOH site and non-H-bonded νOH of the alcohol in each cluster. The spectra of clusters with n = 2 and 3 also show similar spectral features as the cluster with MeOH, when the size of the cluster is the same. The frequencies of all vibrational bands in the 1-NpOH(ROH)$_{2,3}$ are red-shifted in comparison with the non-H-bonded νOH. This indicates that the hydrogen bonding is formed among all OH of 1-NpOH and alcohol. Thus, 1-NpOH(ROH)$_{2,3}$ is suggested to have a ring structure. All of the vibrational bands can be assignable based on an analogy with 1-NpOH(MeOH)$_n$. The assignments are indicated in the figure and are listed in Table 3.

The frequency shifts of H-bonded νOH (1-NpOH) from the monomer is 218, 246, and 280 cm^{-1} in 1-NpOH(MeOH)$_1$, 1-NpOH(EtOH)$_1$, and 1-NpOH(*t*-BuOH)$_1$. The proton affinities of MeOH, EtOH, and *t*-BuOH are 184.9, 190.3, and 195 kcal/mol, respectively.[38] This indicates that there is a positive correlation between the frequency shifts of H-bonded νOH(1-NpOH) and the PA. The frequency shifts of H-bonded νOH-(1-NpOH) are 406, 440, and 456 cm^{-1} in 1-NpOH(MeOH)$_2$, 1-NpOH(EtOH)$_2$, and 1-NpOH(*t*-BuOH)$_2$. Thus, positive correlations of H-bonded νOH(1-NpOH) and the PA have also been found for cluster with n = 2. For n = 3, we cannot discuss the correlation because of the absence of H-bonded νOH(1-NpOH) in the observed region.

Let us discuss the spectral shift of νOH in the solvent molecule. For a cluster with a size of n = 1, the non-H-bonded νOH of the solvent is also shifted to red with increasing alkyl size. The frequency of νOH(ROH) decreases by 12 cm^{-1} when the solvent changes from MeOH to EtOH, while it decreases by 35 cm^{-1} from EtOH to *t*-BuOH. This red shift is attributed to the frequency shift of the solvent, itself, because of the absence of hydrogen bonding for this OH group. The gradual red shift of νOH(ROH) along the alkyl size becomes irregular in a cluster with n = 2. The lower νOH(ROH) is slightly blue shifted when the solvent is changed from EtOH to *t*-BuOH. In a cluster with n = 3, the lowest and highest νOH(ROH) of *t*-BuOH are clearly more blue-shifted than those of EtOH, where the tendency of a gradual red shift is lost. In the size with n = 2 and 3, assuming that they have a ring structure, all OH bonds of the solvent molecule are H-bonded. The frequency-shift of H-bonded νOH is roughly thought to indicate the strength of the hydrogen-bond.[63,64] Thus, the blue shift corresponds to a weaker hydrogen bond when the solvent changes from EtOH to *t*-BuOH, despite the larger PA compared to the MeOH's. The weakened hydrogen bond in 1-NpOH(*t*-BuOH)$_n$ can be understood in terms of the structure. As mentioned in Section III.C., the hydrogen-bonded network in the 1-NpOH-(MeOH)$_n$ is deformed in the ring structure, and the O−H···O hydrogen bond is bent. Assuming that 1-NpOH(*t*-BuOH)$_n$ also

have a ring structure, the deformation is thought to be larger because of the steric hindrance by the alkyl group. Because the hydrogen bond is also bent larger, the weakening of the hydrogen bond, which is indicated by the blue shift of νOH, can be understood.

We have thus learned that steric hindrance plays an important role in the solvation mechanism in 1-NpOH/alcohol clusters. On the basis of this fact, let us discuss the difference in the solvation mechanism between 1-NpOH(MeOH)$_n$ and 1-NpOH-(H$_2$O)$_n$. Here, the latter were previously investigated by combining IR dip spectroscopy and ab initio MO calculations at the MP2/6-31G level,[28] which is the same level as in this work. In a cluster with $n = 1$, both solvents are proton-acceptors, while 1-NpOH is a proton-donor. The O$\cdots$H intermolecular distance in 1-NpOH(MeOH)$_1$ is shorter than that in 1-NpOH(H$_2$O)$_1$ (1.783 Å) by $\sim$0.03 Å (see Figure 3). This indicates that the interaction between molecules in 1-NpOH(MeOH)$_1$ is stronger than in 1-NpOH(H$_2$O)$_1$. This result is consistent with the order of the PA (H$_2$O < MeOH). Contrary to a cluster with $n = 1$, the relation between the intermolecular distance and the PA is broken in larger clusters. Here, both 1-NpOH(H$_2$O)$_{2,3}$ and the 1-NpOH(MeOH)$_{2,3}$ have a ring structure (see Figure 3). The intermolecular distance between 1-NpOH and the solvent accepting the proton of the 1-NpOH in 1-NpOH(MeOH)$_2$ is longer than that in 1-NpOH(H$_2$O)$_2$ (1.723 Å) by $\sim$0.01 Å. The intermolecular distance is not shortened in the 1-NpOH(MeOH)$_3$ cluster compared to 1-NpOH(H$_2$O)$_3$ (the intermolecular distance is 1.615 Å). All other intermolecular distances in 1-NpOH-(MeOH)$_{2,3}$ are larger than in 1-NpOH(H$_2$O)$_{2,3}$. The shorter intermolecular distance of 1-NpOH(MeOH)$_1$ compared to 1-NpOH(H$_2$O)$_1$ indicates that the molecules in 1-NpOH-(MeOH)$_{2,3}$ are well separated by the steric hindrance produced by the alkyl group. The larger steric hindrance may be consistent with the absence of ESPT in 1-NpOH(MeOH)$_n$. The MeOH, itself, has a larger PA than H$_2$O, but the "effective" PA becomes smaller because of the steric hindrance in the cluster. This is the difference in the solvation mechanism between H$_2$O and MeOH.

IV. Conclusion

The R2PI and ion-detected IR dip spectra of the 1-NpOH-(ROH)$_n$ ($n = 1-3$; ROH = MeOH, EtOH, and *t*-BuOH) have been measured. The $S_1 \leftarrow S_0$ mass-selected R2PI spectra of 1-NpOH(ROH)$_n$ showed sharp absorption bands consisting of a strong electronic origin and associated excited-state vibrational excitations. The origin band of 1-NpOH(ROH)$_n$ was monotonically red-shifted with increasing the cluster size. The R2PI spectra of $n = 1$ showed that the origin band was the strongest band, while those of clusters with a larger size showed that higher vibronic bands are more intense than the origin. This indicates a large geometry change of the cluster with increasing cluster size due to $S_1 \leftarrow S_0$ excitation.

The ion-detected IR dip spectra of the 1-NpOH(ROH)$_n$ showed a clear vibrational structure for the H-bonded OH stretching modes in clusters. In 1-NpOH(MeOH)$_n$, the observed IR spectra are compared with the theoretical spectra of various stable conformations predicted by ab initio MO calculations. From a comparison, the vibrational assignments and the geometrical structures of the clusters in the ground state were determined; only the most stable structure for each *n* reproduce the spectral pattern. In the case of $n = 1$, 1-NpOH is a proton donor and MeOH is a proton acceptor. The $n = 2$ and $n = 3$ clusters have a ring structure, where every molecule interacts through a hydrogen bond. Because a ring with the case $n = 2$ is small, the hydrogen-bonded network is deformed, and because a $n = 3$ cluster can form a larger ring than a $n = 2$ cluster, the distortion of the H-bonded network decreases and the interaction among molecules increases. This leads to a red-shift of the bands, corresponding to the OH stretching modes. On the basis of the results for 1-NpOH(MeOH)$_n$, the IR spectra of 1-NpOH-(EtOH)$_n$ and 1-NpOH(*t*-BuOH)$_n$ were analyzed. Because there is a similarity among the IR spectra of 1-NpOH(ROH)$_n$, we have concluded that all three kinds of clusters have the same conformation. We found a positive correlation of the H-bonded νOH(1-NpOH) and the PA of ROH for $n = 1$ and 2. A comparison of the shift of H-bonded νOH(ROH) elucidated the deformation of the H-bonded network by the steric hindrance of the alkyl group in the cases of $n = 2$ and 3. The steric hindrance by the alkyl group is an important factor in the solvation of alcohol.

A structural comparison of 1-NpOH(MeOH)$_n$ and 1-NpOH-(H$_2$O)$_n$ also showed that MeOH is prevented from approaching 1-NpOH in 1-NpOH(MeOH)$_n$. The larger steric hindrance is consistent with the absence of ESPT in 1-NpOH(MeOH)$_n$ clusters.

Acknowledgment. We thank Professor K. Hashimoto for his valuable discussions. This work was financially supported in part by a Grant-in-Aid for Scientific Research from the Ministry of Education, Culture, Sports, Science and Technology (MEXT).

References and Notes

(1) Bartok, W.; Lucchesi, P. J.; Snider N. S. *J. Phys. Chem.* **1961**, *84*, 1842.
(2) Harris, C. M.; Sellnger, B. K. *J. Phys. Chem.* **1980**, *84*, 891.
(3) Webb, S. P.; Philips, L. A.; Yeh, S. W.; Tolbert, L. M.; Clark, J. H. *J. Phys. Chem.* **1986**, *90*, 5154.
(4) Krshnan, R.; Fillingim, T. G.; Lee, J.; Robinson, G. W. *J. Am. Chem. Soc.* **1990**, *112*, 1353.
(5) Pines, E.; Fleming, G. R. *Chem. Phys.* **1994**, *183*, 393.
(6) Smith, D.; Adams, N. G.; Henchman, M. J. *J. Chem. Phys.* **1980**, *72*, 4951.
(7) Harris, C. M.; Sellnger, B. K. *J. Phys. Chem.* **1980**, *84*, 1366.
(8) Föster, T *Z. Elektrochem.* **1950**, *54*, 531.
(9) Weller, A. *Z. Elektrochem.* **1952**, *56*, 662.
(10) Weller, A *Z. Physik. Chem.* **1958**, *17*, 224.
(11) Ireland, J. F.; Wyatt, P. A. H. *Adv. Phys. Org. Chem.* **1976**, *12*, 131.
(12) Huppert, D.; Gutman, M.; Kaufman, K. J. In *Advances in Chemical Physics*; Jortner, J., Levine, R. D., Rice, S. A., Eds.; Wiley-Interscience: New York, 1981; Vol. 47, Part II.
(13) Hercules, D. M.; Rogers, L. B. *Spectrochim. Acta* **1959**, *15*, 393.
(14) Suzuki, S.; Baba, H. *Bull. Chem. Soc. Jpn.* **1967**, *40*, 2199.
(15) Cheshnovsky, O.; Leutwyler, S. *Chem. Phys. Lett.* **1985**, 121, 1.
(16) Knochenmuss, R.; Cheshnovsky, O.; Leutwyler, S. *Chem. Phys. Lett.* **1988**, *144*, 317.
(17) Humpty, S. J.; Pratt, D. W. *J. Chem. Phys.* **1996**, *104*, 8332.
(18) Knochenmuss, R.; Muiño, P. L.; Wickleder, C. *J. Phys. Chem.* **1996**, *100*, 11218.
(19) Knochenmuss, R.; Karbach, V.; Wickleder, C.; Graf, S.; Leutwyler, S. *J. Phys. Chem. A* **1998**, *102*, 1935.
(20) Cheshnovsky, O.; Leutwyler, S. *J. Chem. Phys.* **1988**, *88*, 4127.
(21) Knochenmuss, R.; Leutwyler, S. *J. Chem. Phys.* **1989**, *91*, 1268.
(22) Kim, S. K.; Li. S.; Bernstein, E. R. *J. Chem. Phys.* **1991**, *95*, 3119.
(23) Bürgi, T.; Droz, T.; Leutwyler, S. *Chem. Phys. Lett.* **1995**, *246*, 291.
(24) Knochenmuss, R. *Chem. Phys. Lett.* **1998**, *293*, 191.
(25) Kelley, D. F.; Bernstein, E. R. *Chem. Phys. Lett.* **1999**, *305*, 230.
(26) Knochenmuss, R. *Chem. Phys. Lett.* **1999**, *305*, 233.
(27) Knochenmuss, R. *Chem. Phys. Lett.* **1999**, *311*, 439.
(28) Yoshino, R.; Hashimoto, K.; Omi, T.; Ishiuchi, S.; Fujii, M. *J. Phys. Chem. A* **1998**, *102*, 6227.
(29) Connell, L. L.; Ohline, S. M.; Joireman, P. W.; Corcoran, T. C.; Felker, P. M. *J. Chem. Phys.* **1991**, *94*, 4668.
(30) Breen, J. J.; Peng, L. W.; Willberg, D. M.; Heikai, A.; Cong, P.; Zewail, A. H. *J. Chem. Phys.* **1990**, *92*, 805.

(31) Hineman, M. F.; Brucker, G. A.; Kelley, D. F.; Berstein, E. R. *J. Chem. Phys.* **1992**, *97*, 3341.
(32) Knochenmuss, R.; Holtom, G.; Ray, D. *Chem. Phys. Lett.* **1993**, *215*, 188.
(33) Knochenmuss, R.; Smith, D. E. *J. Chem. Phys.* **1994**, *101*, 7327.
(34) Kim, S. K.; Wang, J.-K.; Zewail, A. H. *Chem. Phys. Lett.* **1994**, *228*, 369.
(35) Syage, J. A. *J. Phys. Chem.* **1995**, *99*, 5772.
(36) Kim, S. K.; Breen, J. J.; Willberg, D. M.; Peng, L. W.; Heikai, A.; Syage, J. A.; Zewail, A. H. *J. Phys. Chem.* **1995**, *99*, 7421.
(37) Lührs, D. C.; Knochenmuss, R.; Fischer, I. *Phys. Chem. Chem. Phys.* **2000**, *2*, 4335.
(38) Aue, D. H.; Bowers, M. T. In *Gas-Phase Ion Chemistry*; Bowers, M. T., Ed.; Academic: New York, 1979; Vol. 2, Chapter 9.
(39) Ebata, T.; Fujii, A.; Mikami, N. *Int. Rev. Phys. Chem.* **1998**, *17*, 331, and references therein.
(40) Robertson, E. G.; Simons, J. P. *Phys. Chem. Chem. Phys.* **2001**, *3*, 1, and references therein.
(41) (a) Riehn, C.; Lahmann, C.; Wassermann, B.; Brutschy, B. *Chem. Phys. Lett.* **1992**, *197*, 443. (b) Brutschy, B. *Chem. Rev.* **2000**, *100*, 3891, and references therein.
(42) Omi, T.; Shitomi, H.; Sekiya, N.; Takazawa, K.; Fujii, M. *Chem. Phys. Lett.* **1996**, *252*, 287.
(43) Frisch, M. J.; Trucks, G. W.; Schlegel, H. B.; Scuseria, G. E.; Robb, M. A.; Cheeseman, J. R.; Zakrzewski, V. G.; Montgomery, J. A., Jr.; Stratmann, R. E.; Burant, J. C.; Dapprich, S.; Millam, J. M.; Daniels, A. D.; Kudin, K. N.; Strain, M. C.; Farkas, O.; Tomasi, J.; Barone, V.; Cossi, M.; Cammi, R.; Mennucci, B.; Pomelli, C.; Adamo, C.; Clifford, S.; Ochterski, J.; Petersson, G. A.; Ayala, P. Y.; Cui, Q.; Morokuma, K.; Malick, D. K.; Rabuck, A. D.; Raghavachari, K.; Foresman, J. B.; Cioslowski, J.; Ortiz, J. V.; Stefanov, B. B.;Liu, G.; Liashenko, A.; Piskorz, P.; Komaromi, I.; Gomperts, R.; Martin, R. L.; Fox, D. J.; Keith, T.; Al-Laham, M. A.; Peng, C. Y.; Nanayakkara, A.; Gonzalez, C.; Challacombe, M.; Gill, P. M. W.; Johnson, B.; Chen, W.; Wong, M. W.; Andres, J. L.; Gonzalez, C.; Head-Gordon, M.; Replogle, E. S.; Pople, A. J. *Gaussian 98*, Revision A.5; Gaussian, Inc.: Pittsburgh, PA, 1998.
(44) Johnson, J. R.; Jordan, K. D.; Plusquellic, D. F.; Pratt, D. W. *J. Chem. Phys.* **1990**, *93*, 2258.
(45) Schütz, M.; Bürgi, T.; Leutwyler, S.; Fischer, T. *J. Chem. Phys.* **1993**, *98*, 3763.
(46) Herzberg, G. *Infrared and Raman Spectra of Polyatomic Molecules*; Van Nostrand Reinhold: Princeton, 1945; p 335.
(47) Djafari, S.; Barth, H. D.; Buchhold, K.; Brutschy, B. *J. Chem. Phys.* **1997**, *107*, 10573.
(48) Barth, H. D.; Buchhold, K.; Djafari, S.; Reimann, B.; Lommatzsch, U.; Brutschy, B. *Chem. Phys.* **1998**, *239*, 49.
(49) Riehn, C.; Buchhold, K.; Reimann, B.; Djafari, S.; Barth, H. D.; Brutschy, B.; Tarakeshwar, P.; Kim, K. S. *J. Chem. Phys.* **2000**, *112*, 1170.
(50) Buchhold, K.; Reimann, B.; Djafari, S.; Barth, H. D.; Brutschy, B.; Tarakeshwar, P.; Kim, K. S. *J. Chem. Phys.* **2000**, *112*, 1844.
(51) Matsumoto, Y.; Ebata, T.; Mikami, N. *J. Chem. Phys.* **1998**, *109*, 6303.
(52) Guchhait, N.; Ebata, T.; Mikami, N. *J. Chem. Phys.* **1999**, *111*, 8438.
(53) Matsumoto, Y.; Ebata, T.; Mikami, N. *J. Mol. Struct.* **2000**, *552*, 257.
(54) Ishiuchi, S.; Saeki, M.; Sakai, M.; Fujii M. *Chem. Phys. Lett.* **2000**, *322*, 27.
(55) Pribble, R. N.; Zwier, T. S. *Faraday Discuss.* **1994**, *97*, 229.
(56) Pribble, R. N.; Hagemeister, F. C.; Zwier, T. S. *J. Chem. Phys.* **1997**, *106*, 2145.
(57) Gruenloh, C. J.; Hagemeister, F. C.; Carney, J. R.; Zwier, T. S. *J. Phys. Chem. A* **1999**, *103*, 503.
(58) Gerhards, M.; Unterberg, C.; Kleinermanns, K. *Phys. Chem. Chem. Phys.* **2000**, *2*, 5538.
(59) Spangenberg, D.; Imhof, P.; Roth, W.; Janzen, C.; Kleinermanns, K. *J. Phys. Chem. A* **1999**, *103*, 5918.
(60) Imhof, P.; Roth, W.; Janzen, C.; Spangenberg, D.; Kleinermanns, K. *Chem. Phys.* **1999**, *242*, 141.
(61) Schmitt, M.; Küpper, J.; Spangenberg, D.; Westphal, A. *Chem. Phys.* **2000**, *254*, 349.
(62) Küpper, J.; Westphal, A.; Schmitt, M. *Chem. Phys.* **2001**, *263*, 41.
(63) Pimentel, G. C.; McClellan, A. L. *The Hydrogen Bond*; Freeman, W. H. and Co.: San Francisco, 1960; pp 82−85.
(64) Thompson, W. H.; Hynes, J. T. *J. Am. Chem. Soc.* **2000**, *122*, 6278.